

Archon: A Unified Multimodal Model for Holistic Digital Human Generation

Chong Bao^{1,2*§} Shichen Liu^{2*} Lijun Yu³ David Futschik² Stylianos Moschoglou²
 Shefali Srivastava² Ziqian Bai² Feitong Tan² Guofeng Zhang¹
 Zhaopeng Cui¹ Sean Fanello² Yinda Zhang^{2†}
¹State Key Lab of CAD&CG, Zhejiang University ²Google ³Google DeepMind

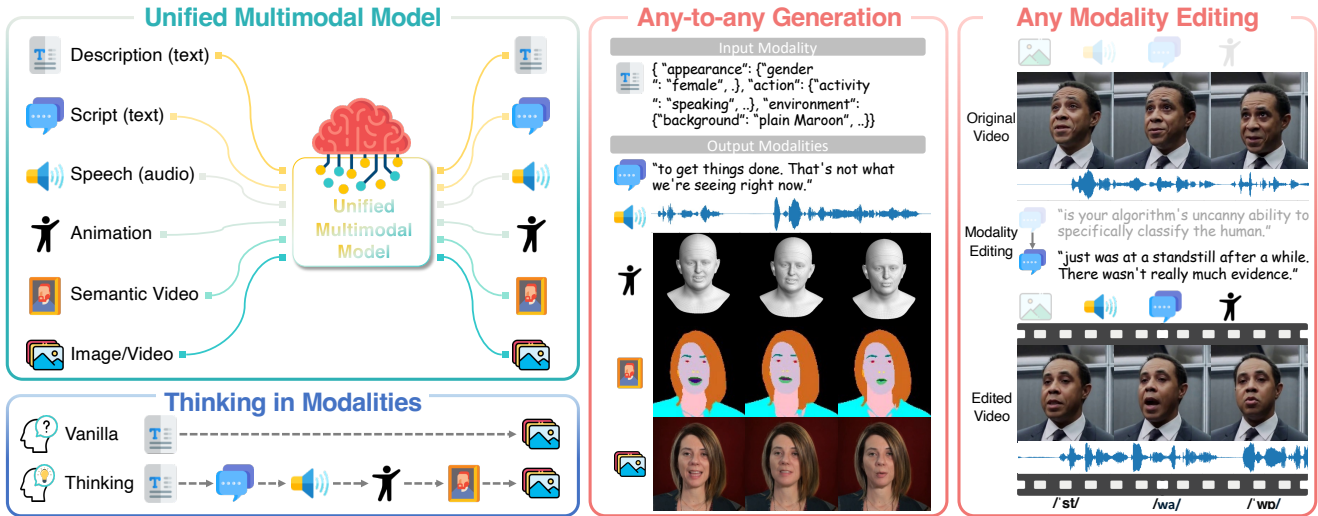


Figure 1. **Archon**. We propose a novel unified multimodal model that performs cross-modal generation among a wide range of modalities, including description, script, speech, animation, semantic video, image, and video. Furthermore, we introduce the concept of *Thinking in Modality* to reduce ambiguity during cross-modal transitions and enhance generation quality. Our model inherently supports conditional generation across arbitrary sets of modalities, enabling any modality editing throughout the entire multimodal input space.

Abstract

Digital humans are fundamental to immersive interaction, yet creating a unified model for holistic modalities, including text, audio, motion, and visual content, remains an open challenge. In this paper, we present Archon, a fully pretrained, human-centric unified multimodal model for holistic avatar generation. Archon unifies seven modalities with modality-specific tokenizers, and a native autoregressive unified multimodal model pretrained on synchronized modalities and 72 diverse tasks to model holistic joint distributions. To address the token explosion challenge in high-fidelity talking videos, we introduce a memory-efficient semantic video reparameterization achieving 4× token reduction while preserving fine-grained dynamics, coupled with a semantic-driven video diffusion decoder. We further propose a “Thinking in Modality” that decomposes

ambiguous cross-modal tasks into stepwise thinking in an alternative chain of modality, progressively enhancing fidelity and controllability. Extensive experiments demonstrate that Archon achieves superior or comparable performance across diverse digital human generation tasks, validating the effectiveness of our unified framework. Project page: <https://zju3dv.github.io/archon/>.

1. Introduction

Digital humans are central to modern human–computer interaction, virtual reality, and digital entertainment. To support faithful representation, engaging communication, and flexible interaction, a unified model is required to seamlessly integrate a rich set of perceptual modalities, including text, audio, motion, semantic and color, capable of processing and generating each signal on demand. Despite decades of progress, creating fine-grained controllable digital humans that is able to process holistic multimodal signals remains a significant open challenge.

* Authors contributed equally.

† Corresponding authors.

§ The work was done during an internship at Google.

Current approaches for digital human systems are largely built upon specialized expert models that target individual modalities or sub-tasks, such as speech-driven video generation [8, 12, 35, 43, 51, 58, 65, 68] and image-conditioned text-to-speech [20, 25, 29, 59]. While these approaches achieve impressive realism within their respective domains, they share fundamental limitations: fragmentation and inefficiency. Training on distinct, modality-specific datasets introduces distribution mismatches, making the coordination of different expert models as a unified system brittle for novel multimodal tasks. This fragmentation also leads to redundant capacity and limited scalability, as each expert model must independently learn task-specific knowledge that could otherwise be shared in a modality-driven unified space. Crucially, the introduction of any new modality demands training a new model from scratch or non-trivial finetuning of a model designed for a different task. In contrast, we advocate for a holistic, unified, *any-to-any* multimodal generative framework that overcomes these issues by reusing shared representations and seamlessly adapting to novel tasks without requiring dedicated model pretraining.

Existing unified multimodal models are not truly “holistic” in the context of digital humans. While current multimodal language models (MLLM) [2, 4, 9, 32, 36, 44, 57] focus on understanding multimodal inputs, their outputs are confined to text. Conversely, contemporary unified generative models can generate text, image or video but overlook the supports on audio [15, 55, 56, 63, 67], or generate only non-speech audio such as music or environmental sounds [28, 55, 63]. Specifically for digital human, parsing human speech, animation (e.g., through 3D Morphable Model), and preserving identity across the temporal dimension are barely studied in the domain of multimodal models.

To address these challenges, we introduce Archon, a pretrained unified multimodal model designed for holistic digital human generation. Archon pushes general-purpose multimodal reasoning to domain-specific avatar synthesis, enabling holistic cross-modal generation and understanding across a comprehensive set of modalities, including description, speech (transcript and audio), animation, semantic video, image, and video. First, we design a suite of modality-specific tokenizers that encode heterogeneous signals from each modality into discrete integer tokens, which are subsequently merged into a unified vocabulary. These tokenizers are crafted to balance reconstruction fidelity with token-sequence efficiency, facilitating compact yet expressive representations across modalities. Second, we propose a native unified multimodal model that models the joint distribution of holistic modalities in a autoregressive framework. To support large-scale pretraining, we curate a comprehensive multimodal dataset comprising synchronized modality pairs and 72 diverse multimodal tasks, enabling the model to learn rich cross-modal correspondences.

Third, human-centric talking videos inherently involve high-frequency dynamics, such as lip motion, facial expressions, and head poses, which demand high frame rates (e.g., 30 fps). However, a 5-second 30 fps video at 256×256 resolution amounts to 9K tokens [61], exceeding the context window of MLLMs (8K tokens) [3]. Moreover, MLLM’s reasoning on discrete tokens disrupts the continuous nature of video signals, thereby degrading generation quality. To overcome this, we introduce a memory-efficient video discretization tailored for cross-modal reasoning, coupled with a semantic-driven video diffusion decoder for high-fidelity video synthesis. Specifically, we replace RGB videos with semantic videos, which consist of discrete semantic labels and preserve essential dynamics and structure while discarding redundant visual information, achieving a 4× reduction in token count. Subsequently, a video diffusion model conditioned on semantic video, reference images, and textual descriptions generates high-quality videos.

Fourth, certain cross-modal generation tasks suffer from substantial domain gaps and inherent ambiguities. For instance, generating video from speech necessitates both extracting explicit information (e.g., gender) and synthesizing missing details (e.g., appearance, expression), which challenges the scaling-to-quality rule of expert models. Leveraging the flexibility of our unified model in holistic cross-modal reasoning, we introduce a “Thinking in Modality” strategy during inference. This approach decomposes complex cross-modal tasks into stepwise thinking in an alternative chain of modality generation, progressively enhancing fidelity and controllability in cross-modal synthesis.

Our contributions can be summarized as:

- We introduce Archon, a fully pretrained, human-centric unified multimodal model with holistic avatar synthesis via a native MLLM pretrained on synchronized modalities and 72 tasks to model holistic joint distributions.
- We propose a memory-efficient video discretization and a semantic-driven diffusion decoder for efficient and high-quality generation, and a “Thinking in Modality” inference strategy to enhance fidelity and controllability.
- Extensive experiments demonstrate superior or comparable performance with expert models across holistic digital human generation tasks, validating the effectiveness of our unified framework.

2. Related Works

Digital human generation. Research on digital humans has evolved from modality-specific modeling towards increasingly unified representations. Early studies focused on specialized tasks, such as facial modeling and reconstruction from images [13, 19], talking heads generation and lip synchronization from audio [8, 12, 51, 52, 65], personalized speech generation from identity [29], and similar isolated tasks. While these expert systems achieved high fidelity

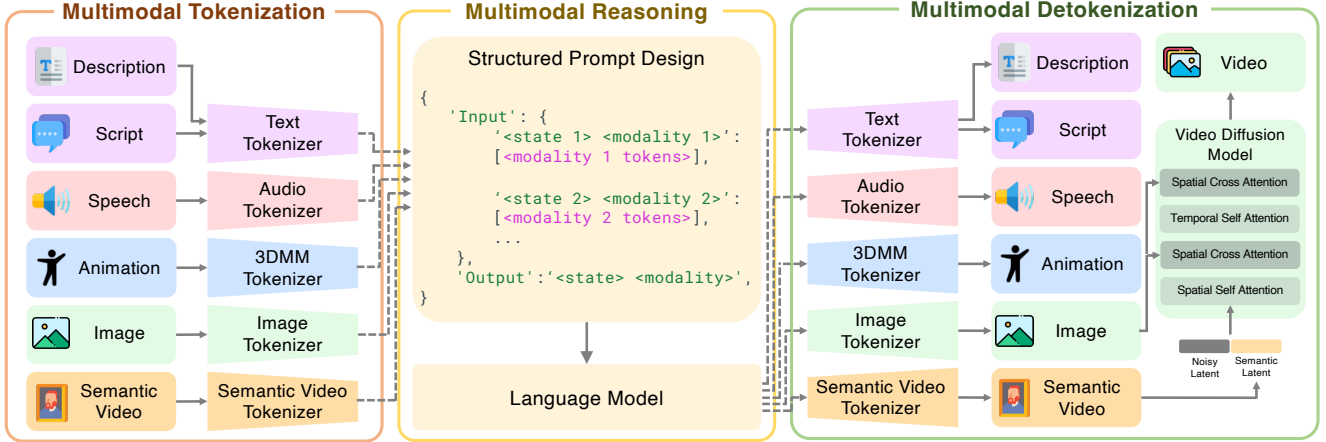


Figure 2. **Pipeline.** We use modality tokenizers to tokenize description, script, speech, animation, image and semantic video into discrete tokens. These tokens are arranged in a structured format and input to the language model for multimodal reasoning. The synthesized tokens are detokenized into raw modalities. For synthesizing high-quality video, we employ a semantic-driven video diffusion model to synthesize high-quality video conditioned on image and semantic segmentations.

within their domains, they typically rely on task-specific model architecture, limiting cross-modal generalization. To overcome these constraints, more recent efforts aim to couple multiple tasks or modalities into unified human-centric frameworks. Human foundation models such as Sapiens [26] and OmniHuman [31] move toward large-scale representations pretraining that jointly capture pose, geometry, and semantic understanding, while promptHMR [50] introduces language-guided controllability in mesh recovery. Despite advances, most existing systems still treat inputs or outputs as modality-specific, rather than learning a truly unified interface across modalities. Consequently, these systems struggle with any-to-any modality translation. **Multimodal language models.** In parallel, multimodal models [15, 28, 55, 63] demonstrate that diverse data types can be represented within a unified transformer backbone. Models such as Flamingo [2], PaLM-E [16], and Kosmos [36] extend language models with multimodal context, improving cross-modal reasoning and conditional generation. The development of modality-specific discrete tokenizers [38, 60–62] further enables unified sequence modeling across text, audio, video, and other signals. This paradigm is explored by AudioLM [6], SpeechGPT [64], VideoPoet [28], and large unified architectures such as Gemini [44], showing that a single transformer can perform both perception and generation through a shared token space. Building on these insights, we extend unified multimodal model into the domain of avatar.

3. Method

We propose a unified multimodal model for holistic digital human generation and understanding. As shown in

Fig. 2, our model consists of four core modules: (1) a set of modality-specific tokenizers (Sec. 3.1), (2) a language model backbone for cross-modal reasoning (Sec. 3.2), (3) a semantic-driven diffusion model for high-quality video generation (Sec. 3.3), (4) “Thinking in Modality” strategy for high quality and controllability generation (Sec. 3.4).

3.1. Multimodal Tokenization

As shown in Fig. 2, we model a comprehensive coverage of modalities in the digital human, which are *description*, *script*, *speech*, *animation*, *semantic video*, *image* and *video*. In the following paragraphs, we introduce the tokenization process of each modality. The details of the model architectures and training strategies are in supplementary Sec. D.

Image tokenizer. We employ the pretrained MAGVIT-v2 [61] model for image tokenization, selected for its superior visual fidelity and compression capabilities. MAGVIT-v2 [61] is a 3D convolution-based VQGAN [18] that utilizes a lookup-free vocabulary with a codebook size of 2^{18} . We leverage this model to quantize images of 256×256 resolution into a discrete 16×16 token representation.

Semantic video as context-efficient video tokenizer. Directly adopting existing video tokenizers [61] is impractical in multimodal model, as their token output often exceeds the context window capacity of language models. As a case in point, a 32GB-HBM TPUv6 can accommodate a context window of approximately 8K tokens. However, encoding a five-second, 256×256 video (30 fps) produces 9K tokens [61]. Furthermore, the sheer magnitude of video tokens introduces a severe modality imbalance. A five-second audio clip, for instance, generates only 940 tokens, representing a small fraction of the video token count. This discrepancy leads to a training bias, as video tokens

overwhelmingly dominate the dataset. Naïve token reduction via higher-compression tokenizers is infeasible, as this necessitates retraining a new tokenizer with an intractably large vocabulary (exceeding 2^{18}) and network bottleneck, which in turn significantly increases the language model’s modality learning complexity.

Inspired by semantic-to-video generation works [33], we introduce a novel, memory-efficient discretization strategy that decomposes the video into a reference image and a semantic video. The reference image is typically the first video frame. The semantic video comprises 21 discrete semantic categories (e.g., eyelid, eyebrow, nose) obtained from an off-the-shelf face segmentation model [34]. The semantic video retains crucial structural and motion information while discarding texture, significantly reducing the information density but preserving the pixel-domain nature of the video. The discrete nature of the semantic labels induces a smooth distribution along the spatial dimension and aligns naturally with the autoregressive reasoning paradigm of large language models, which allows a low-resolution semantic video to effectively represent a high-resolution video. A video diffusion model is subsequently used to up-sample and generate a high-quality video conditioned on the semantic video and reference image (detailed in Sec. 3.3).

Specifically, we learn a semantic video tokenizer to compress a $L \times 128 \times 128$ semantic video into $(\frac{L-1}{4} + 1) \times 8 \times 8$ tokens, where L is the number of frames. We finetune MAGVIT-v2 [61] to reuse its powerful pretrained encoders. An *invertible color embedding* is defined to map each semantic label to a distinct RGB color, allowing the semantic video to be processed as a standard color video. To align with the reduced complexity of this representation, the codebook size of our semantic tokenizer is set to 2^{10} .

Speech tokenizer. We use a pretrained SoundStream tokenizer [62] for speech tokenization. SoundStream [62] employs a residual vector quantizer (RVQ) that encodes 16 kHz audio into discrete tokens at 25 frames per second across 8 residual levels. Following the VideoPoet [28], we retain only the first 4 RVQ levels for efficiency and stability. Each of these residual levels has an independent vocabulary of 1,024 codes. The final token sequence is constructed by arranging tokens from lower to higher levels, preserving the hierarchical structure of the residual quantization.

Animation tokenizer. We utilize 3D Morphable Model (3DMM) parameters [30] to parameterize the animation of digital humans. The 3DMM have three components: shape, expression, and pose. The shape parameters capture the subject’s static geometry and appearance, remaining invariant throughout the video clip, and are represented by an e_{sh} -dimensional vector. In contrast, the expression and pose parameters evolve temporally and are modeled as continuous 1D temporal signals, with respective dimensions of $L \times e_{exp}$ and $L \times e_{pose}$. We independently learn three Residual Vec-

tor Quantized VAE (VQVAE) models [46] for shape, expression and pose. Each employs causal convolution to discretize parameters. The resulting codebooks are configured as follows: shape (8 levels, 512 codes per level), expression (8 levels, 2048 codes per level), and pose (6 levels, 512 codes per level). Consistent with the speech tokens, the final RVQ token sequence is constructed by arranging tokens from lower to higher residual levels.

Text tokenizer. To preserve the inherent text generation capabilities of our language model, we retain its original tokenizer, the T5 encoder [39], for all text processing tasks.

3.2. Language Model for Multimodal Generation

We employ an auto-regressive language model that supports flexible generation by conditioning on prompts contextualized with task and modality-specific token cues.

Task definition. Different from typical multimodal settings that focus on only a few generation tasks, the input and output of the holistic digital human generation problem can be arbitrary modality sets. We categorize the modalities of interest into *time-dependent* ones $D_{var} = \{d_{scr}, d_{spc}, d_{exp}, d_{sem}, d_{vid}\}$, including *script*, *speech*, *semantic masks*, and *video*; and *time-invariant* ones $D_{inv} = \{d_{img}, d_{dsc}, d_{shp}\}$, including *image*, *description*, and *shape*. We define the full modality set as

$$\mathcal{D} = \{d^t \mid d \in D_{var}^t, t \in \{0, 1\}\} \cup D_{inv}, \quad (1)$$

where d^0, d^1 denote the modality in the past and present tense respectively. Given input modalities $\mathcal{D}_{cond} \subset \mathcal{D}$ as conditions, the goal of a generation task is to generate a subset of the remaining modalities $T : \mathcal{D}_{cond} \rightarrow \mathcal{D}_{gen}$, where $\mathcal{D}_{gen} = \{d_j \mid d_j \notin \mathcal{D}_{cond}\}$. Existing works [28, 49] employ a special task token to instruct the task type. However, as the number of modalities increases, the possible combinations of input and output causes combinatorial explosion, making it increasingly difficult for the model to handle all tasks within a unified framework. To address this challenge, we reformulate the auto-regressive generation process allowing an arbitrary combination as

$$T_j : \begin{cases} \mathcal{D}_{cond} \rightarrow d_1, & j = 1, \\ \mathcal{D}_{cond} \cup \{d_1, \dots, d_{j-1}\} \rightarrow d_j, & j > 1. \end{cases} \quad (2)$$

This recurrent formulation makes explicit that, at each step j , the model generates one modality d_j conditioned on the input modalities along with all previously generated ones. Consequently, rather than training the model to generate all modalities jointly, we train it to predict *one modality at a time*. This reduction preserves the expressive power of the original formulation while substantially simplifying the task space. For clarity, we henceforth define sequential generation order from d_1 to $d_{|\mathcal{D}_{gen}|}$ as $\mathcal{D}_{cond} \rightarrow [d_1, \dots, d_{|\mathcal{D}_{gen}|}]$.

Prompt design. To instruct the model of input and desired output, the input prompt, which is a series of tokens, must

contain necessary task information. Existing language models [3, 9, 11, 21] are good at parsing and understanding the structured inputs, e.g., HTML, JSON, etc. Rather than employing special tokens to denote modalities or tasks, we organize the prompt as a structured data serialization filled with natural language descriptors. These descriptors serve as keys that explicitly delineate the modality type, state, input, and expected output, as illustrated in Fig. 2. This design has two advantages: (1) it mitigates the burden of the model that heavily relies on a sparse set of special tokens; (2) it provides clearer semantic grounding that can leverage the knowledge in the pretrained language model.

Language model backbone. We adopt PaLM2 [3], a prefix decoder-only model with bidirectional prefix attention. The model processes an input sequence of tokens and autoregressively predicts the subsequent token from a unified vocabulary. This vocabulary partitions different modalities into distinct contiguous index ranges; for instance, text tokens occupy indices 0–256127, while video tokens are assigned to 256128–518272. Each token is associated with its own learnable embedding vector.

Multimodal training strategy. To equip our model with the ability to map across arbitrary modality sets, we conduct training across 72 diverse multimodal tasks and enable compositional inference (see supplementary Sec. C.3 for details). Following the AGD training paradigm [1], we employ a context window of 8K tokens, dynamically populated at each training step by sampling from our task distribution. However, a naive random sampling approach, selecting one task per step, is susceptible to three forms of training bias: (1) Model bias, where gradients backpropagate towards a sub-optimal direction for a single-modality task rather than the global gradient for multiple modality tasks. (2) Distributional bias, where random sampling over an uneven task distribution causes the model to under-prioritize modalities with fewer tasks. (3) Difficulty variance, where tasks of greater difficulty intrinsically require more learning effort. To overcome these challenges, we first sample multiple tasks at each step, ensuring the model learns the joint distribution of multiple modalities. Second, we propose a novel sampling strategy to balance the multimodal training, factoring in both the task count per modality and the task difficulty. The sampling weight $S(i)$ for the i -th task is defined as: $S(i) = \frac{\log(p_i)}{N_{m(i)}}$ where p_i is the perplexity of the i -th task, and $N_{m(i)}$ is the total number of tasks with the output modality being $m(i)$. The perplexity p_i measures task difficulty and estimated using a baseline model trained with uniform sampling weights. This strategy balances model capacity to learn joint distribution across all tasks.

3.3. Semantic-driven Video Diffusion Model

While the language model leverages discrete semantic videos as a memory-efficient alternative to continuous RGB



Figure 3. **Thinking in Modality.** We show the results of speech-to-video generation with different thinking strategies. The videos generated from chain 2 contain less distortion (e.g., blurry appearance and undefined textual symbols) and exhibit closer identity alignment with the ground truth.

videos for cross-modal reasoning, we introduce a semantic-driven video diffusion model that decodes these semantic videos into high-fidelity outputs, guided by a reference image and textual description.

Semantic and appearance conditioning. We employ WALT [23], a transformer-based latent diffusion model originally designed for text-to-video generation, as our video diffusion backbone. We modify its architecture to accept low-resolution reference images, semantic masks, and textual descriptions as inputs for high-quality video generation. To provide strong motion guidance, we concatenate the encoded semantic mask latents with the noisy video latents along the feature dimension before feeding them into the diffusion model. We utilize a cross-attention module to condition the reference image. To enhance the correspondence between video latents and the reference image, we extract the semantic mask of the reference image and concatenate its encoded semantic latent with the reference image latent along the feature dimension, analogous to our semantic signal conditioning. This composite feature is then concatenated with text embeddings to perform cross-attention with the video latent. In this way, semantics serves as a structural bridge, facilitating the effective transmission of the reference appearance into the generated video.

Diffusion training. We fine-tune the entire WALT [23] backbone to adapt it for our semantic-driven video generation task. The input reference images and semantic masks are processed at 256×256 resolution, while the output videos are synthesized at 512×512 resolution. The model employs a v-prediction parameterization [40] and is optimized using Mean Squared Error (MSE) loss between the predicted and target velocities.

3.4. Thinking in Modality

While our model supports direct generation between modalities, we observe that different modality transitions exhibit varying levels of uncertainty. For instance, generating video directly from speech typically shows higher perplexity than

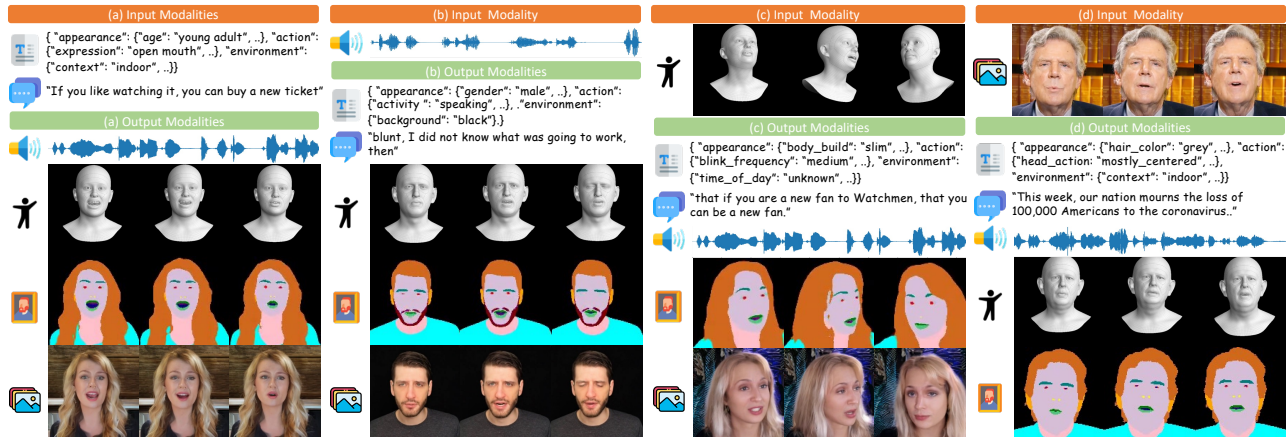


Figure 4. **Multimodal Generation.** We show holistic modality generation and understanding given an arbitrary modality as input.

from 3DMM shape and expression, as shown in Fig. 3, indicating that the latter offers a more controllable and interpretable pathway. Motivated by this, we introduce *thinking in modality* — an inference strategy that explores alternative generative chains by instructing the model to produce intermediate modalities that form a smooth transition in semantic granularity, thereby reducing uncertainty and improving output quality. This approach requires no retraining and simply exploits the model’s ability to condition on multiple modalities in a unified framework.

4. Experiments

4.1. Experiment Setup

Models. We fine-tune a pretrained 1B PaLM2 [3] featuring a 550K vocabulary to equip the model with the language priors. The vocabulary size of language model is 550K for multimodal tokens. We employed the Adam optimizer [27] with a weight decay of 10^{-3} and a 4,000-step learning rate warmup from 0 to 10^{-3} , followed by a cosine decay schedule to 5×10^{-5} . We use 256 TPUv6 Trillium to train the language model for 20 days with a batch size of 256. For the diffusion model, we employ Adafactor optimizer [41] and a 6,000-step linear warmup from 0 to 1.2×10^{-4} followed by a constant schedule. We use 128 TPUv6 to train the diffusion model for 10 days with batch size 128.

Datasets. We train our model on a comprehensive multimodal dataset with 6,000 hours of monologue videos sourced from the public Internet. Each video contains speech and script synchronized to the video [10]. We caption the video with Gemini 2.5 Pro [11], fit the 3DMM parameters following [53], and extract the face segmentation using our trained segmentation models with a DinoV2 backbone [34]. We evaluate our method on two standard benchmarks: CelebV-HQ [69] and HDTF [66] that are disjoint from our training dataset. From each, we randomly sample a test set of 200 videos following previous work [8, 12], and

extract the script from the speech using Whisper [37].

4.2. Multimodal Generation and Editing

Multimodal generation. We demonstrate our model’s any-to-any generation capabilities in Fig. 4. First, we showcase text-to-all generation. Given a description of a person’s appearance, action, and environment, optionally augmented with a script, our model sequentially generates all corresponding modalities: script, speech, 3DMM, segmentation, and the talking video. As shown in Fig. 4(a), our model generates realistic talking videos of a woman, with speech and visuals that precisely adhere to the input attributes. Second, for speech-to-all generation, our model infers the person’s appearance (as a description) and script from the input speech, subsequently using these to generate the talking video, 3DMM, and segmentation. As illustrated in Fig. 4(b), the model correctly interprets the person’s gender from the audio and generates a video that is temporally synchronized with the input speech. Third, our model supports more fine-grained control using 3DMM or segmentation as inputs. When conditioned on these signals, it convincingly generates high-fidelity videos with responsive head motion and accurate expressions that match the input, as shown in Fig. 4(c). Finally, our model exhibits a strong capacity for understanding high-level modalities from low-level video, semantic, and 3DMM inputs. As shown in Fig. 4(d), our model extract a description of the person’s appearance, action, and environment; read the script directly from lip motion (lip-reading); synthesize a semantically-coherent voice for the input signals; reconstruct the 3DMM coefficients and semantic segmentations from the input video. Please see supplementary Sec. E.1 for more examples.

Modality-specific editing. We demonstrate the modality-specific editing capability of our model in Fig. 5. Firstly, we showcase script editing in Fig. 5(a). Our model synthesizes new speech following the edited script in the original voice

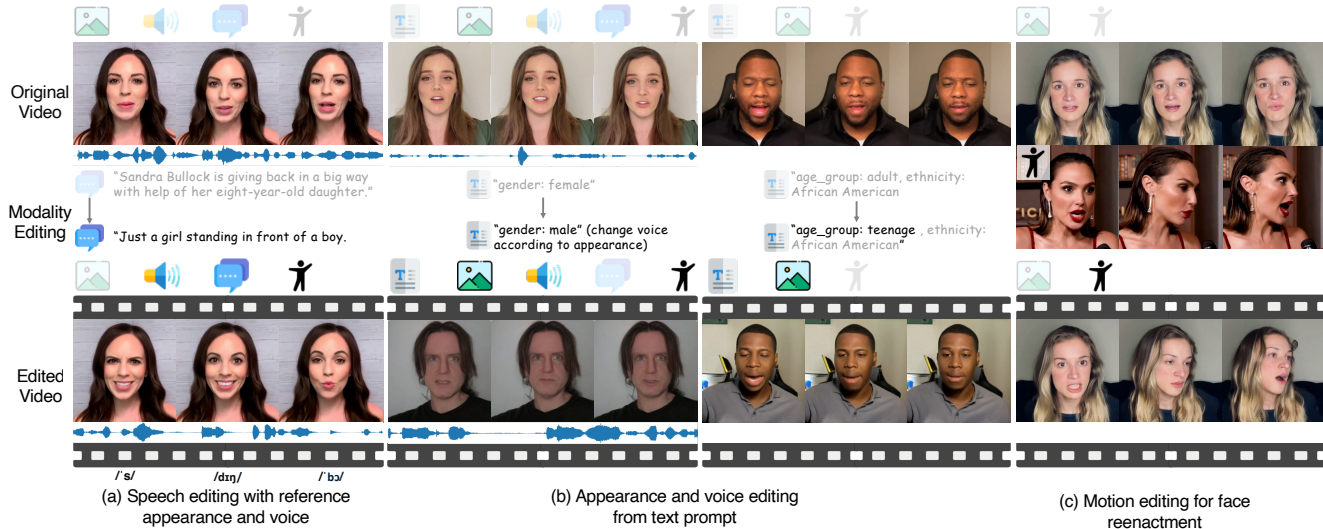


Figure 5. **Modality-specific Editing.** We show flexible any modality editing to modify an arbitrarily chosen modality while maintain the others untouched. The icons on the top show the modalities used in the example, and the highlighted icons are the ones that are edited.

and new video with synchronized lip motion and animation while maintain the identity. Secondly, our model can seamlessly change the appearance of the subject via text prompt. As shown in Fig. 5(b), changing the gender or appearance attributes in the text description synthesizes a new talking video, retaining all other original aspects. The speech is optionally modified to match the new appearance while still following the original script. Finally, we perform face reenactment by editing the head motion using a reference video, as shown in Fig. 5(c). Our model generates high-quality videos with animation aligned with the reference, even under extreme head poses.

4.3. Comparisons on Modality-Specific Tasks

Although our model is built for broad multimodal generation, we investigate its performance on canonical modality-specific benchmarks to assess the unified architecture’s capability in handling individual tasks. Note that our multimodal model is not trained on the benchmark dataset and is used straightforward on these tasks without any finetuning.

Baselines. We conduct a comparative analysis against state-of-the-art across two tasks: (1) *Audio-driven video generation*: We compare our model against AniPortrait [52], Echomimic [8], and Hallo3 [8]. (2) *Image-conditioned text-to-speech*: We compare our model against FaceTTS [29].

Metrics. We employ a suite of metrics targeting video quality, lip synchronization, and audio fidelity. We measure the perceptual distributional distance between generated and ground truth videos using Fréchet Inception Distance (FID) [24] and Fréchet Video Distance (FVD) [45], and assess video quality using Q-Align VLM (IQA) [54]. We quantify lip-sync accuracy using the confidence (Sync-C) and distance (Sync-D) scores from the pre-trained Sync-

Methods	CelebV-HQ [69]				
	FID↓	FVD↓	Sync-C↑	Sync-D↓	IQA↑
AniPortrait* [52]	39.73	160.7	3.493	10.982	3.833
EchoMimic* [8]	56.81	236.9	4.463	9.575	3.601
Hallo3 [12]	<u>15.67</u>	<u>105.5</u>	5.429	<u>9.158</u>	3.722
Ours	6.818	93.81	<u>5.210</u>	8.998	<u>3.794</u>

Methods	HDTF [66]				
	FID↓	FVD↓	Sync-C↑	Sync-D↓	IQA↑
AniPortrait [52]	42.03	162.8	2.879	10.889	3.813
EchoMimic* [8]	45.90	241.6	5.467	9.36	3.743
Hallo3* [12]	<u>12.78</u>	<u>96.51</u>	6.376	<u>9.131</u>	<u>3.83</u>
Ours	5.779	81.64	<u>6.198</u>	8.822	3.94

Table 1. **Comparisons on speech-driven video generation.** We compare video generation quality and lip synchronization against baselines. “*” denotes methods trained on the benchmark dataset.

Methods	CelebV-HQ [69]			HDTF [66]		
	MCD-DTW↓	C-SIM↑	Id. Acc.↑	MCD-DTW↓	C-SIM↑	Id. Acc.↑
FaceTTS	7.9383	0.9048	0.6032	7.8128	0.8844	0.5715
Ours	8.918	0.9117	0.6223	8.9822	0.9002	0.5911

Table 2. **Comparisons on image-conditioned text-to-speech.** We compare speech quality and voice-identity coherence against the FaceTTS [29].

Net model [10]. For audio fidelity, we use Mel Cepstral Distortion with Dynamic Time Warping (MCD-DTW) [5] to measure the audio quality, and cosine similarity (C-SIM) [42, 48] to measure the voice identity coherence.

Speech-driven video generation. We provide quantitative comparisons in Tab. 1. Our model surpasses all baselines on FID and FVD, indicating superior video quality and alignment with the ground truth. Moreover, our model yields lip synchronization and IQA scores that are comparable to established strong baselines, including Echomimic [8] and Hallo3 [12] that are specifically trained on the benchmark



Figure 6. **Comparison on the Speech-driven Video Generation.** We qualitatively compare the video quality and video-audio synchronization against AniPortrait [52], Echomimic [8], Hallo3 [12].

datasets. This notable performance highlights the exceptional quality of our lip synchronization and overall realism. We further provide qualitative comparisons in Fig. 6. Notably, given an image of a woman with closed eyes (Fig. 6 left), our method and Echomimic successfully synthesize the woman opening her eyes and speaking, whereas AniPortrait [52] and Hallo3 fail to achieve this. We also observe that Hallo3 tends to synthesize exaggerated expressions on accented notes (Fig. 1 right). While this boosts Syn-C score, the resulting expressions often appear unnatural. In contrast, our method not only synthesizes a high-quality video with a consistent identity, but also generates realistic lip motions highly synchronized to the accompanying speech.

Image-conditioned speech generation. Quantitative results are detailed in Tab. 2. Our model achieves superior performance on C-SIM and Identity Accuracy across both datasets, confirming better identity coherence and stronger semantic matching between the reference image and the generated audio identity. This enhanced identity-to-audio mapping is a direct result of our multimodal training strategy. However, we observe a slightly lower MCD-DTW score, primarily because our model adopts a lightweight, general-purpose detokenizer, while FaceTTS [29] employs a heavier audio diffusion model tailored to this task.

4.4. Ablation Studies

Unified vs. modality-specific modeling. To examine the capacity efficiency of unified multimodal modeling, we compare our model against a baseline composed of multiple expert models, with each producing a single modality trained with identical data, architecture, and training settings. The total parameter count across all experts is set to match that of our unified model. As shown in Tab. 3, the unified model outperforms the ensemble of experts

Methods	CelebV-HQ [69]				
	FID↓	FVD↓	Sync-C↑	Sync-D↓	IQA↑
w/o Unified Model	7.279	170	3.209	10.143	3.695
w/o Thinking	13.76	128.1	3.088	10.209	3.593
Full Model	6.818	93.81	5.210	8.998	3.794

Methods	HDTF [66]				
	FID↓	FVD↓	Sync-C↑	Sync-D↓	IQA↑
w/o Unified Model	6.353	199.5	3.991	9.97	3.892
w/o Thinking	13.43	110.3	4.478	9.597	3.809
Full Model	5.779	81.64	6.198	8.822	3.94

Table 3. **Ablation on Design Choices.** We show ablation studies of different designs on speech-driven video generation task.

across all metrics. This indicates that jointly learning across modalities within a shared architecture yields stronger representations than training isolated experts models.

Effect of thinking-in-modality. We perform quantitative and qualitative ablations on our modality thinking strategy. As shown in Tab. 3, we compare two variants for speech-driven video generation. *W/o Thinking* directly generates $\{d_{\text{sph}}, d_{\text{img}}\} \rightarrow [d_{\text{vid}}]$, whereas *Full Model* utilizes the full chain of generation: $\{d_{\text{sph}}, d_{\text{img}}\} \rightarrow [d_{\text{shp}}, d_{\text{exp}}, d_{\text{sem}}, d_{\text{dsc}}, d_{\text{vid}}]$. Our *Full Model* surpasses the baseline on all metrics, demonstrating that incorporating 3DMM and description as intermediate representations stabilizes video quality and audio synchronization.

5. Conclusion

We present Archon, a unified multimodal model for holistic digital human generation. Archon supports any-modality-to-any generation, understanding, and editing across description, script, speech, animation, semantic video, image, and video. Archon is a step toward truly unified digital human modeling, where diverse modalities coexist and interact coherently within a single generative framework. Please refer to supplementary Sec. B for more discussions.

References

- [1] Hassan Akbari, Dan Kondratyuk, Yin Cui, Rachel Hornung, Huisheng Wang, and Hartwig Adam. Alternating gradient descent and mixture-of-experts for integrated multimodal perception. *Advances in Neural Information Processing Systems*, 36:79142–79154, 2023. 5
- [2] Jean-Baptiste Alayrac, Jeff Donahue, Pauline Luc, Antoine Miech, Iain Barr, Yana Hasson, Karel Lenc, Arthur Mensch, Katherine Millican, Malcolm Reynolds, et al. Flamingo: a visual language model for few-shot learning. *Advances in neural information processing systems*, 35:23716–23736, 2022. 2, 3
- [3] Rohan Anil, Andrew M Dai, Orhan Firat, Melvin Johnson, Dmitry Lepikhin, Alexandre Passos, Siamak Shakeri, Emanuel Taropa, Paige Bailey, Zhifeng Chen, et al. Palm 2 technical report. *arXiv preprint arXiv:2305.10403*, 2023. 2, 5, 6
- [4] Shuai Bai, Yuxuan Cai, Ruizhe Chen, Keqin Chen, Xionghui Chen, Zesen Cheng, Lianghao Deng, Wei Ding, Chang Gao, Chunjiang Ge, Wenbin Ge, Zhifang Guo, Qidong Huang, Jie Huang, Fei Huang, Binyuan Hui, Shutong Jiang, Zhaohai Li, Mingsheng Li, Mei Li, Kaixin Li, Zicheng Lin, Junyang Lin, Xuejing Liu, Jiawei Liu, Chenglong Liu, Yang Liu, Dayiheng Liu, Shixuan Liu, Dunjie Lu, Ruilin Luo, Chenxu Lv, Rui Men, Lingchen Meng, Xuancheng Ren, Xingzhang Ren, Sibao Song, Yuchong Sun, Jun Tang, Jianhong Tu, Jianqiang Wan, Peng Wang, Pengfei Wang, Qiuyue Wang, Yuxuan Wang, Tianbao Xie, Yiheng Xu, Haiyang Xu, Jin Xu, Zhibo Yang, Mingkun Yang, Jianxin Yang, An Yang, Bowen Yu, Fei Zhang, Hang Zhang, Xi Zhang, Bo Zheng, Humen Zhong, Jingren Zhou, Fan Zhou, Jing Zhou, Yuanzhi Zhu, and Ke Zhu. Qwen3-vl technical report. *arXiv preprint arXiv:2511.21631*, 2025. 2
- [5] Eric Battenberg, RJ Skerry-Ryan, Soroosh Mariooryad, Daisy Stanton, David Kao, Matt Shannon, and Tom Bagby. Location-relative attention mechanisms for robust long-form speech synthesis. In *ICASSP 2020-2020 IEEE International Conference on Acoustics, Speech and Signal Processing (ICASSP)*, pages 6194–6198. IEEE, 2020. 7
- [6] Zalán Borsos, Raphaël Marinier, Damien Vincent, Eugene Kharitonov, Olivier Pietquin, Matt Sharifi, Dominik Roblek, Olivier Teboul, David Grangier, Marco Tagliasacchi, et al. Audioldm: a language modeling approach to audio generation. *IEEE/ACM transactions on audio, speech, and language processing*, 31:2523–2533, 2023. 3
- [7] Jianlv Chen, Shitao Xiao, Peitian Zhang, Kun Luo, Defu Lian, and Zheng Liu. Bge m3-embedding: Multilingual, multi-functionality, multi-granularity text embeddings through self-knowledge distillation, 2023. 19
- [8] Zhiyuan Chen, Jiajiong Cao, Zhiquan Chen, Yuming Li, and Chenguang Ma. Echomimic: Lifelike audio-driven portrait animations through editable landmark conditions. In *Proceedings of the AAAI Conference on Artificial Intelligence*, pages 2403–2410, 2025. 2, 6, 7, 8
- [9] Aakanksha Chowdhery, Sharan Narang, Jacob Devlin, Maarten Bosma, Gaurav Mishra, Adam Roberts, Paul Barham, Hyung Won Chung, Charles Sutton, Sebastian Gehrmann, et al. Palm: Scaling language modeling with pathways. *Journal of Machine Learning Research*, 24(240): 1–113, 2023. 2, 5
- [10] Joon Son Chung and Andrew Zisserman. Out of time: automated lip sync in the wild. In *Asian conference on computer vision*, pages 251–263. Springer, 2016. 6, 7
- [11] Gheorghe Comanici, Eric Bieber, Mike Schaekermann, Ice Pasupat, Noveen Sachdeva, Inderjit Dhillon, Marcel Blstein, Ori Ram, Dan Zhang, Evan Rosen, et al. Gemini 2.5: Pushing the frontier with advanced reasoning, multimodality, long context, and next generation agentic capabilities. *arXiv preprint arXiv:2507.06261*, 2025. 5, 6, 15
- [12] Jiahao Cui, Hui Li, Yun Zhan, Hanlin Shang, Kaihui Cheng, Yuqi Ma, Shan Mu, Hang Zhou, Jingdong Wang, and Siyu Zhu. Hallo3: Highly dynamic and realistic portrait image animation with diffusion transformer networks. *arXiv e-prints*, pages arXiv–2412, 2024. 2, 6, 7, 8
- [13] Radek Daněček, Michael J Black, and Timo Bolkart. Emoca: Emotion driven monocular face capture and animation. In *Proceedings of the IEEE/CVF Conference on Computer Vision and Pattern Recognition*, pages 20311–20322, 2022. 2, 17
- [14] Google Deepmind. Gemini 3. <https://deepmind.google/models/gemini/>, 2025. 19
- [15] Chaorui Deng, Deyao Zhu, Kunchang Li, Chenhui Gou, Feng Li, Zeyu Wang, Shu Zhong, Weihao Yu, Xiaonan Nie, Ziang Song, et al. Emerging properties in unified multimodal pretraining. *arXiv preprint arXiv:2505.14683*, 2025. 2, 3
- [16] Danny Driess, Fei Xia, Mehdi SM Sajjadi, Corey Lynch, Aakanksha Chowdhery, Brian Ichter, Ayzaan Wahid, Jonathan Tompson, Quan Vuong, Tianhe Yu, et al. Palme: An embodied multimodal language model. *arXiv preprint arXiv:2303.03378*, 2023. 3
- [17] Bernhard Egger, William AP Smith, Ayush Tewari, Stefanie Wuhrer, Michael Zollhoefer, Thabo Beeler, Florian Bernard, Timo Bolkart, Adam Kortylewski, Sami Romdhani, et al. 3d morphable face models—past, present, and future. *ACM Transactions on Graphics (ToG)*, 39(5):1–38, 2020. 17
- [18] Patrick Esser, Robin Rombach, and Bjorn Ommer. Taming transformers for high-resolution image synthesis. In *Proceedings of the IEEE/CVF conference on computer vision and pattern recognition*, pages 12873–12883, 2021. 3, 13
- [19] Yao Feng, Haiwen Feng, Michael J Black, and Timo Bolkart. Learning an animatable detailed 3d face model from in-the-wild images. *ACM Transactions on Graphics (ToG)*, 40(4): 1–13, 2021. 2
- [20] Shunsuke Goto, Kotaro Onishi, Yuki Saito, Kentaro Tachibana, and Koichiro Mori. Face2speech: Towards multi-speaker text-to-speech synthesis using an embedding vector predicted from a face image. In *Interspeech*, pages 1321–1325, 2020. 2
- [21] Aaron Grattafiori, Abhimanyu Dubey, Abhinav Jauhri, Abhinav Pandey, Abhishek Kadian, Ahmad Al-Dahle, Aiesha Letman, Akhil Mathur, Alan Schelten, Alex Vaughan,

- et al. The llama 3 herd of models. *arXiv preprint arXiv:2407.21783*, 2024. 5
- [22] Robert Gray. Vector quantization. *IEEE Assp Magazine*, 1(2):4–29, 1984. 14
- [23] Agrim Gupta, Lijun Yu, Kihyuk Sohn, Xiuye Gu, Meera Hahn, Fei-Fei Li, Irfan Essa, Lu Jiang, and José Lezama. Photorealistic video generation with diffusion models. In *European Conference on Computer Vision*, pages 393–411. Springer, 2024. 5
- [24] Martin Heusel, Hubert Ramsauer, Thomas Unterthiner, Bernhard Nessler, and Sepp Hochreiter. Gans trained by a two time-scale update rule converge to a local nash equilibrium. *Advances in neural information processing systems*, 30, 2017. 7
- [25] Minki Kang, Wooseok Han, and Eunho Yang. Facestylespeech: Improved face-to-voice latent mapping for natural zero-shot speech synthesis from a face image. *arXiv preprint arXiv:2311.05844*, 2023. 2
- [26] Rawal Khirodkar, Timur Bagautdinov, Julieta Martinez, Su Zhaoen, Austin James, Peter Selednik, Stuart Anderson, and Shunsuke Saito. Sapiens: Foundation for human vision models. In *European Conference on Computer Vision*, pages 206–228. Springer, 2024. 3
- [27] Diederik Kinga, Jimmy Ba Adam, et al. A method for stochastic optimization. In *International conference on learning representations (ICLR)*. California, 2015. 6
- [28] Dan Kondratyuk, Lijun Yu, Xiuye Gu, José Lezama, Jonathan Huang, Grant Schindler, Rachel Hornung, Vighnesh Birodkar, Jimmy Yan, Ming-Chang Chiu, et al. Videopoet: A large language model for zero-shot video generation. *arXiv preprint arXiv:2312.14125*, 2023. 2, 3, 4
- [29] Jiyoung Lee, Joon Son Chung, and Soo-Whan Chung. Imaginary voice: Face-styled diffusion model for text-to-speech. In *ICASSP 2023-2023 IEEE International Conference on Acoustics, Speech and Signal Processing (ICASSP)*, pages 1–5. IEEE, 2023. 2, 7, 8
- [30] Tianye Li, Timo Bolkart, Michael J Black, Hao Li, and Javier Romero. Learning a model of facial shape and expression from 4d scans. *ACM Trans. Graph.*, 36(6):194–1, 2017. 4
- [31] Gaojie Lin, Jianwen Jiang, Jiaqi Yang, Zerong Zheng, Chao Liang, Yuan Zhang, and Jingtuo Liu. Omnihuman-1: Rethinking the scaling-up of one-stage conditioned human animation models. In *Proceedings of the IEEE/CVF International Conference on Computer Vision*, pages 13847–13858, 2025. 3
- [32] Haoyu Lu, Wen Liu, Bo Zhang, Bingxuan Wang, Kai Dong, Bo Liu, Jingxiang Sun, Tongzheng Ren, Zhuoshu Li, Hao Yang, et al. Deepseek-vl: towards real-world vision-language understanding. *arXiv preprint arXiv:2403.05525*, 2024. 2
- [33] Arun Mallya, Ting-Chun Wang, Karan Sapra, and Ming-Yu Liu. World-consistent video-to-video synthesis. In *European Conference on Computer Vision*, pages 359–378. Springer, 2020. 4
- [34] Maxime Oquab, Timothée Darcet, Théo Moutakanni, Huy Vo, Marc Szafranec, Vasil Khalidov, Pierre Fernandez, Daniel Haziza, Francisco Massa, Alaaeldin El-Nouby, et al. Dinov2: Learning robust visual features without supervision. *arXiv preprint arXiv:2304.07193*, 2023. 4, 6, 17
- [35] Youxin Pang, Yong Zhang, Weize Quan, Yanbo Fan, Xiaodong Cun, Ying Shan, and Dong-ming Yan. Dpe: Disentanglement of pose and expression for general video portrait editing. In *Proceedings of the IEEE/CVF Conference on Computer Vision and Pattern Recognition*, pages 427–436, 2023. 2
- [36] Zhiliang Peng, Wenhui Wang, Li Dong, Yaru Hao, Shaohan Huang, Shuming Ma, and Furu Wei. Kosmos-2: Grounding multimodal large language models to the world. *arXiv preprint arXiv:2306.14824*, 2023. 2, 3
- [37] Alec Radford, Jong Wook Kim, Tao Xu, Greg Brockman, Christine McLeavey, and Ilya Sutskever. Robust speech recognition via large-scale weak supervision. In *International conference on machine learning*, pages 28492–28518. PMLR, 2023. 6, 17
- [38] Colin Raffel, Noam Shazeer, Adam Roberts, Katherine Lee, Sharan Narang, Michael Matena, Yanqi Zhou, Wei Li, and Peter J. Liu. Exploring the limits of transfer learning with a unified text-to-text transformer. *Journal of Machine Learning Research*, 21(140):1–67, 2020. 3
- [39] Colin Raffel, Noam Shazeer, Adam Roberts, Katherine Lee, Sharan Narang, Michael Matena, Yanqi Zhou, Wei Li, and Peter J Liu. Exploring the limits of transfer learning with a unified text-to-text transformer. *Journal of machine learning research*, 21(140):1–67, 2020. 4
- [40] Tim Salimans and Jonathan Ho. Progressive distillation for fast sampling of diffusion models. *arXiv preprint arXiv:2202.00512*, 2022. 5
- [41] Noam Shazeer and Mitchell Stern. Adafactor: Adaptive learning rates with sublinear memory cost. In *International Conference on Machine Learning*, pages 4596–4604. PMLR, 2018. 6
- [42] David Snyder, Daniel Garcia-Romero, Gregory Sell, Daniel Povey, and Sanjeev Khudanpur. X-vectors: Robust dnn embeddings for speaker recognition. In *2018 IEEE international conference on acoustics, speech and signal processing (ICASSP)*, pages 5329–5333. IEEE, 2018. 7
- [43] Shuai Tan, Bill Gong, Bin Ji, and Ye Pan. Fixtalk: Taming identity leakage for high-quality talking head generation in extreme cases. *arXiv preprint arXiv:2507.01390*, 2025. 2
- [44] Gemini Team, Rohan Anil, Sebastian Borgeaud, Jean-Baptiste Alayrac, Jiahui Yu, Radu Soricut, Johan Schalkwyk, Andrew M Dai, Anja Hauth, Katie Millican, et al. Gemini: a family of highly capable multimodal models. *arXiv preprint arXiv:2312.11805*, 2023. 2, 3
- [45] Thomas Unterthiner, Sjoerd Van Steenkiste, Karol Kurach, Raphael Marinier, Marcin Michalski, and Sylvain Gelly. Towards accurate generative models of video: A new metric & challenges. *arXiv preprint arXiv:1812.01717*, 2018. 7
- [46] Aaron Van Den Oord, Oriol Vinyals, et al. Neural discrete representation learning. *Advances in neural information processing systems*, 30, 2017. 4
- [47] Aaron Van Den Oord, Oriol Vinyals, et al. Neural discrete representation learning. *Advances in neural information processing systems*, 30, 2017. 14, 17

- [48] Li Wan, Quan Wang, Alan Papir, and Ignacio Lopez Moreno. Generalized end-to-end loss for speaker verification. In *2018 IEEE International Conference on Acoustics, Speech and Signal Processing (ICASSP)*, pages 4879–4883. IEEE, 2018. 7
- [49] Wenhai Wang, Zhe Chen, Xiaokang Chen, Jiannan Wu, Xizhou Zhu, Gang Zeng, Ping Luo, Tong Lu, Jie Zhou, Yu Qiao, et al. Visionllm: Large language model is also an open-ended decoder for vision-centric tasks. *Advances in Neural Information Processing Systems*, 36:61501–61513, 2023. 4
- [50] Yufu Wang, Yu Sun, Priyanka Patel, Kostas Daniilidis, Michael J Black, and Muhammed Kocabas. Promptmhr: Promptable human mesh recovery. In *Proceedings of the Computer Vision and Pattern Recognition Conference*, pages 1148–1159, 2025. 3
- [51] Cong Wei, Bo Sun, Haoyu Ma, Ji Hou, Felix Juefei-Xu, Zecheng He, Xiaoliang Dai, Luxin Zhang, Kunpeng Li, Tingbo Hou, et al. Mocha: Towards movie-grade talking character synthesis. *arXiv preprint arXiv:2503.23307*, 2025. 2
- [52] Huawei Wei, Zejun Yang, and Zhisheng Wang. Aniportrait: Audio-driven synthesis of photorealistic portrait animation. *arXiv preprint arXiv:2403.17694*, 2024. 2, 7, 8
- [53] Erroll Wood, Tadas Baltrušaitis, Charlie Hewitt, Sebastian Dziadzio, Thomas J Cashman, and Jamie Shotton. Fake it till you make it: face analysis in the wild using synthetic data alone. In *Proceedings of the IEEE/CVF international conference on computer vision*, pages 3681–3691, 2021. 6
- [54] Haoning Wu, Zicheng Zhang, Weixia Zhang, Chaofeng Chen, Liang Liao, Chunyi Li, Yixuan Gao, Annan Wang, Erli Zhang, Wenxiu Sun, et al. Q-align: Teaching llms for visual scoring via discrete text-defined levels. *arXiv preprint arXiv:2312.17090*, 2023. 7
- [55] Shengqiong Wu, Hao Fei, Leigang Qu, Wei Ji, and Tat-Seng Chua. Next-gpt: Any-to-any multimodal llm. In *Forty-first International Conference on Machine Learning*, 2024. 2, 3, 18, 19
- [56] Jinheng Xie, Zhenheng Yang, and Mike Zheng Shou. Show-o2: Improved native unified multimodal models. *arXiv preprint arXiv:2506.15564*, 2025. 2, 18
- [57] Jin Xu, Zhifang Guo, Hangrui Hu, Yunfei Chu, Xiong Wang, Jinzheng He, Yuxuan Wang, Xian Shi, Ting He, Xinfu Zhu, Yuanjun Lv, Yongqi Wang, Dake Guo, He Wang, Linhan Ma, Pei Zhang, Xinyu Zhang, Hongkun Hao, Zishan Guo, Baosong Yang, Bin Zhang, Ziyang Ma, Xipin Wei, Shuai Bai, Keqin Chen, Xuejing Liu, Peng Wang, Mingkun Yang, Dayiheng Liu, Xingzhang Ren, Bo Zheng, Rui Men, Fan Zhou, Bowen Yu, Jianxin Yang, Le Yu, Jingren Zhou, and Junyang Lin. Qwen3-omni technical report. *arXiv preprint arXiv:2509.17765*, 2025. 2, 18
- [58] Sicheng Xu, Guojun Chen, Yu-Xiao Guo, Jiaolong Yang, Chong Li, Zhenyu Zang, Yizhong Zhang, Xin Tong, and Baining Guo. Vasa-1: Lifelike audio-driven talking faces generated in real time. *Advances in Neural Information Processing Systems*, 37:660–684, 2024. 2
- [59] Jiaxin Ye, Boyuan Cao, and Hongming Shan. Emotional face-to-speech. *arXiv preprint arXiv:2502.01046*, 2025. 2
- [60] Lijun Yu, Yong Cheng, Kihyuk Sohn, José Lezama, Han Zhang, Huiwen Chang, Alexander G Hauptmann, Ming-Hsuan Yang, Yuan Hao, Irfan Essa, et al. Magvit: Masked generative video transformer. In *Proceedings of the IEEE/CVF Conference on Computer Vision and Pattern Recognition*, pages 10459–10469, 2023. 3
- [61] Lijun Yu, José Lezama, Nitesh Bharadwaj Gundavarapu, Luca Versari, Kihyuk Sohn, David Minnen, Yong Cheng, Agrim Gupta, Xiuye Gu, Alexander G Hauptmann, et al. Language model beats diffusion-tokenizer is key to visual generation. In *ICLR*, 2024. 2, 3, 4, 12
- [62] Neil Zeghidour, Alejandro Luebs, Ahmed Omran, Jan Skoglund, and Marco Tagliasacchi. Soundstream: An end-to-end neural audio codec. *IEEE/ACM Transactions on Audio, Speech, and Language Processing*, 30:495–507, 2021. 3, 4, 17
- [63] Jun Zhan, Junqi Dai, Jiasheng Ye, Yunhua Zhou, Dong Zhang, Zhigeng Liu, Xin Zhang, Ruibin Yuan, Ge Zhang, Linyang Li, et al. Anygpt: Unified multimodal llm with discrete sequence modeling. In *Proceedings of the 62nd Annual Meeting of the Association for Computational Linguistics (Volume 1: Long Papers)*, pages 9637–9662, 2024. 2, 3
- [64] Dong Zhang, Shimin Li, Xin Zhang, Jun Zhan, Pengyu Wang, Yaqian Zhou, and Xipeng Qiu. Speechgpt: Empowering large language models with intrinsic cross-modal conversational abilities. In *The 2023 Conference on Empirical Methods in Natural Language Processing*, 2023. 3
- [65] Wenxuan Zhang, Xiaodong Cun, Xuan Wang, Yong Zhang, Xi Shen, Yu Guo, Ying Shan, and Fei Wang. Sadtalker: Learning realistic 3d motion coefficients for stylized audio-driven single image talking face animation. In *Proceedings of the IEEE/CVF conference on computer vision and pattern recognition*, pages 8652–8661, 2023. 2
- [66] Zhimeng Zhang, Lincheng Li, Yu Ding, and Changjie Fan. Flow-guided one-shot talking face generation with a high-resolution audio-visual dataset. In *Proceedings of the IEEE/CVF conference on computer vision and pattern recognition*, pages 3661–3670, 2021. 6, 7, 8, 17, 19
- [67] Chunting Zhou, Lili Yu, Arun Babu, Kushal Tirumala, Michihiro Yasunaga, Leonid Shamis, Jacob Kahn, Xuezhe Ma, Luke Zettlemoyer, and Omer Levy. Transfusion: Predict the next token and diffuse images with one multi-modal model. *arXiv preprint arXiv:2408.11039*, 2024. 2
- [68] Hang Zhou, Yasheng Sun, Wayne Wu, Chen Change Loy, Xiaogang Wang, and Ziwei Liu. Pose-controllable talking face generation by implicitly modularized audio-visual representation. In *Proceedings of the IEEE/CVF conference on computer vision and pattern recognition*, pages 4176–4186, 2021. 2
- [69] Hao Zhu, Wayne Wu, Wentao Zhu, Liming Jiang, Siwei Tang, Li Zhang, Ziwei Liu, and Chen Change Loy. Celebv-hq: A large-scale video facial attributes dataset. In *European conference on computer vision*, pages 650–667. Springer, 2022. 6, 7, 8, 17

Supplementary Material

This supplementary material provides additional implementation details, experimental results and a brief discussion on ethics. In Sec. A, we claim that our work adheres to ethical guidelines. In Sec. C, we elaborate on the architectural designs and training protocols for our semantic and animation tokenizers, followed by the detailed specifications of our multimodal task formulation. Sec. D describes the data acquisition and preprocessing pipelines employed for each modality, including description, script, speech, animation, semantic video and video. Finally, Sec. E presents extended qualitative results showcasing multimodal generation and editing capabilities, alongside further quantitative ablation studies on the semantic-guided video diffusion model.

A. Ethical Considerations

We acknowledge the dual-use nature of high-fidelity avatar generation. While promising for telepresence and content creation, this technology carries risks. We strictly condemn the misuse of our work for harassment or misinformation and emphasize that this research is intended solely for academic purposes. We utilize data in strict adherence to their licenses. We are fully committed to the Ethics Guidelines, advocating for safeguards like invisible watermarking and continuous bias monitoring to ensure responsible deployment.

B. Discussion

Archon employs semantic video as a memory-efficient intermediate representation to compress redundant visual information from RGB frames for cross-modal reasoning. To reconstruct high-quality video output, a semantic-driven diffusion model decodes the semantic sequence under the conditioning of a textual description. This design enables the synthesis of vivid, fine-grained facial dynamics, such as frowning and forehead wrinkles, that are not explicitly encoded in the semantic masks, as illustrated in the left examples of Fig. G, while also supporting rich, film-grade emotional expression as shown on the right. Moving forward, the semantic representation could be substituted with more detailed, memory-efficient alternatives to capture subtler visual cues. Furthermore, the expressiveness and diversity of avatars may be enhanced by fine-tuning the model on high-quality cinematic datasets. Additionally, while Archon currently generates single-speaker talking videos, multi-turn dialogues, where only one person appears per frame and

different persons speak one-by-one, could be realized by integrating an external agent system that parses conversation turns and iteratively queries the model with alternating speaker identities for each turn. Generating multiple persons within the same frame simultaneously, however, would require fine-tuning on dedicated multi-person datasets.

C. Implementation Details

C.1. Semantic Video Tokenizer

Model Architecture. Our semantic tokenizer is built upon a 3D convolutional encoder-decoder architecture, designed to map a semantic video to discrete latent codes. The architecture is fully convolutional, consisting of an encoder, a decoder, and look-up free quantizer. We initialize our model’s weights from a pre-trained MAGVIT-v2 [61] checkpoint and introduce a key architectural modification to achieve a higher spatial compression rate suitable for semantic tokenization. Specifically, we add an additional downsampling operation at the beginning of the encoder. This is implemented as a 3D convolution with a spatial stride of 2, which immediately halves the spatial resolution ($H \times W$) of the input video. Correspondingly, a final upsampling block is added at the end of the decoder to restore the original resolution. This modification doubles the spatial downsampling factor of the feature maps before they are quantized, leading to a more compressed grid of semantic tokens. The detailed architectures of the encoder and decoder are presented in Table D and Table E, respectively.

The encoder processes an input video tensor of shape $T \times H \times W \times C_{in}$. It begins with a $3 \times 3 \times 3$ 3D convolution with a stride of (1, 2, 2), halving the spatial dimensions (H, W) from the outset. This is followed by a series of downsampling stages. Each stage consists of multiple residual blocks (ResBlocks) followed by a downsampling layer, which is a strided 3D convolution that reduces spatial resolution and, in some stages, temporal resolution. The number of feature channels is progressively increased through the encoder. The final stage consists of additional ResBlocks and a $1 \times 1 \times 1$ convolution to project the features into the desired embedding dimension, D_{emb} , before quantization.

The decoder is architecturally symmetric to the encoder. It takes the quantized latent tensor of shape $T' \times H' \times W' \times D_{emb}$ and reconstructs the video to its original dimensions. It begins with a $3 \times 3 \times 3$ convolution and several ResBlocks. Subsequently, a series of upsampling stages, each comprising multiple ResBlocks and an upsampling layer, progres-

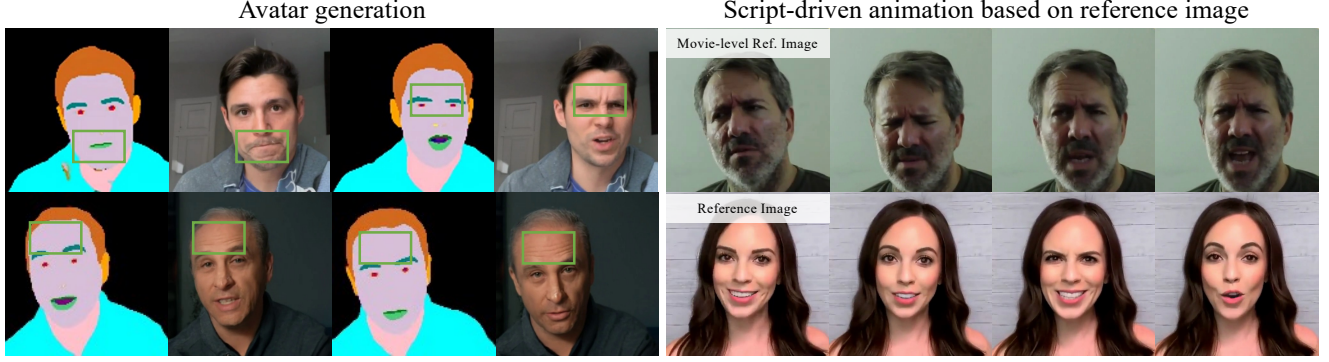


Figure G. **Micro-expression and rich motion generation.** Qualitative results are presented for video generation from textual inputs and script-driven image animation.

Layer	Kernel / Stride	Output Shape	Output Channels
Input	-	$T \times H \times W$	C_{in}
Conv3D (Strided)	$(3, 3, 3) / (1, 2, 2)$	$T \times \frac{H}{2} \times \frac{W}{2}$	F
For $i = 0$ to $N_{blocks} - 1$: (Downsampling Stage i)			
$N_{res} \times$ ResBlock	$(3, 3, 3) / (1, 1, 1)$	$T_i \times H_i \times W_i$	$F \cdot M_i$
Downsample Conv3D	$(4, 4, 4) / (S_{t,i}, 2, 2)$	$T_{i+1} \times H_{i+1} \times W_{i+1}$	$F \cdot M_{i+1}$
$N_{res} \times$ ResBlock	$(3, 3, 3) / (1, 1, 1)$	$T' \times H' \times W'$	$F \cdot M_{last}$
Group Norm + SiLU	-	$T' \times H' \times W'$	$F \cdot M_{last}$
Conv3D (to Embedding)	$(1, 1, 1) / (1, 1, 1)$	$T' \times H' \times W'$	D_{emb}

Table D. The architecture of our 3D CNN Encoder. The input video has dimensions $T \times H \times W \times C_{in}$. F is the base number of filters, M_i are the channel multipliers for each block, N_{res} is the number of residual blocks per stage, and $S_{t,i}$ is the temporal stride for the i -th downsampling layer.

Layer	Kernel / Stride	Output Shape	Output Channels
Input (Quantized Latent)	-	$T' \times H' \times W'$	D_{emb}
Conv3D	$(3, 3, 3) / (1, 1, 1)$	$T' \times H' \times W'$	$F \cdot M_{last}$
$N_{res} \times$ ResBlock	$(3, 3, 3) / (1, 1, 1)$	$T' \times H' \times W'$	$F \cdot M_{last}$
For $i = N_{blocks} - 2$ down to 0: (Upsampling Stage i)			
$N_{res} \times$ ResBlock	$(3, 3, 3) / (1, 1, 1)$	$T_{i+1} \times H_{i+1} \times W_{i+1}$	$F \cdot M_{i+1}$
Upsample + Conv3D	$(3, 3, 3) / (1, 1, 1)$	$T_i \times H_i \times W_i$	$F \cdot M_i$
Group Norm + SiLU	-	$T \times \frac{H}{2} \times \frac{W}{2}$	F
Upsample + Conv3D	$(3, 3, 3) / (1, 1, 1)$	$T \times H \times W$	F
Conv3D (to Output)	$(3, 3, 3) / (1, 1, 1)$	$T \times H \times W$	C_{out}

Table E. The architecture of our 3D CNN Decoder. The input is the latent tensor of shape $T' \times H' \times W' \times D_{emb}$.

sively increase the spatial and temporal resolution while decreasing the number of channels. Upsampling is performed using nearest-neighbor interpolation followed by a $3 \times 3 \times 3$ convolution. To mirror the encoder’s design, the final layer of the decoder is an upsampling block that doubles the spatial resolution, followed by a final convolution to produce

the output video with C_{out} channels.

Training. The model is trained as a VQ-GAN [18], fine-tuning from the aforementioned MAGVIT-v2 checkpoint. The training was conducted on 4 TPU v4 platform and took 140 hours to complete. We train on clips at a 128×128

spatial resolution, with a batch size of 8. The training objective is a composite loss function designed to produce high-fidelity reconstructions that also align with ground-truth semantic segmentation maps. The overall loss function \mathcal{L} is defined as:

$$\mathcal{L} = \mathcal{L}_{\text{recon}} + \lambda_{\text{adv}}\mathcal{L}_{\text{adv}} + \mathcal{L}_{\text{commit}} + \lambda_{\text{seg}}\mathcal{L}_{\text{seg}} \quad (3)$$

where the components are as follows: $\mathcal{L}_{\text{recon}}$ is L2 reconstruction loss between the original semantic video x and the reconstructed semantic video \hat{x} . \mathcal{L}_{adv} is the adversarial loss from a patch-based temporal discriminator that encourages perceptual realism. We set the adversarial loss weight λ_{adv} to 0.3. $\mathcal{L}_{\text{commit}}$ is the commitment loss from the vector quantization layer, which regularizes the latent embedding space. \mathcal{L}_{seg} is a pixel-wise cross-entropy loss between the reconstructed output and the ground-truth segmentation map. The logits for this loss are derived from the negative squared L2 distance between the generated pixel colors and a predefined 21-class color palette, sharpened by a temperature $\tau = 10$. This loss component is crucial for learning a semantic representation, and we set its weight λ_{seg} to 3.0. The model is trained end-to-end using the Adam optimizer with a cosine learning rate schedule and a warm-up phase.

C.2. 3DMM Tokenizer

We develop three distinct tokenizers for identity, expression, and pose respectively, which are fundamental components of a 3D facial parametric model. Each tokenizer is an autoencoder trained using a vector quantization objective (VQ-VAE [47]). While they operate on different input features, they share the same underlying network architecture. Below, we detail this architecture and the training procedure for each tokenizer.

Model Architecture. Our animation tokenizer is a fully convolutional autoencoder that operates on 1D temporal sequences of animation parameters. The architecture consists of an encoder, a decoder, and a Residual Vector Quantizer (RVQ) [22]. The encoder maps the input sequence to a compressed latent representation, which is then quantized by the RVQ. The decoder reconstructs the original sequence from the quantized latents. The encoder and decoder are symmetric and built upon a series of 1D convolutional layers and residual blocks (ResBlocks). The specific configuration is detailed in Table F. The architecture is consistent across all three tokenizers, with the only variation being the input and output feature dimensions.

Training. The three tokenizers for identity, expression, and pose are trained independently on their respective data streams. First, each set of animation parameters (expression, identity, and pose) is normalized independently. We compute the mean and standard deviation for each parameter dimension across the entire training dataset. Then, for

each sample, we subtract the mean and divide by the standard deviation. This standardizes the distribution of each parameter, which is essential for stable training of the subsequent quantization model. Second, the training objective is to minimize the reconstruction error, regularized by the vector quantization loss. The total loss function is a weighted sum of an L2 reconstruction loss and a VQ commitment loss, as defined in the original VQ-VAE work. All models are trained using the AdamW optimizer with a cosine learning rate schedule, including a warm-up phase over the first 0.5% of training steps. The base learning rate is set to 4×10^{-4} . The training is performed using 128 TPU v2. The specific hyperparameters for each tokenizer are detailed below:

- **Identity Tokenizer:** Trained for 200k steps with a global batch size of 1024. The RVQ consists of 12 codebooks, each with a size of 512. The reconstruction loss weight is 50.0, and the commitment loss weight is 1.0.
- **Expression Tokenizer:** Trained for 200k steps with a global batch size of 1024. The RVQ uses 8 codebooks, each of size 2048. The loss weights are the same as for the identity tokenizer.
- **Pose Tokenizer:** Trained for 100k steps with a larger global batch size of 1024 to stabilize training. The RVQ has 12 codebooks, each with a size of 512. The loss weights are the same as for the identity tokenizer.

C.3. Multimodal Task Formulation and Training

Our primary objective is to train a single, versatile multimodal model capable of holistic avatar generation. This necessitates that the model understands and generates the wide array of modalities that constitute a digital avatar. To this end, we have meticulously designed a comprehensive suite of 72 multimodal tasks. These tasks are structured to teach the model not only to generate individual modalities but also to understand the intricate relationships and dependencies between them, enabling a cohesive and realistic generation of a holistic avatar.

The model is trained on a rich set of modalities, encompassing textual (*description*, *script*), acoustic (*speech*), semantic (*semantic*), and a hierarchical set of visual modalities (*identity*, *expression*, *pose*, *image*). Modalities such as *identity*, *image*, and *description* are considered time-invariant. The other modalities can be either from *past* or *current* depending on if they are the conditions or the predictions in task definition.

Our training tasks are formulated as sequence-to-sequence problems, where the model is given a set of input modalities and is asked to generate a target output modality. The tasks can be categorized as follows:

- **Continuation Tasks:** These tasks involve predicting the *current* state of a modality given its *past* state (e.g.,

Layer	Output Shape	Details
Encoder		
Input	$T \times C_{in}$	C_{in}
Conv1D	$T \times F$	kernel=3, stride=1
Stage 1	$T/2 \times F$	$2 \times \text{ResBlock}(F)$, Downsample
Stage 2	$T/4 \times F$	$2 \times \text{ResBlock}(F)$, Downsample
Stage 3	$T/4 \times F$	$2 \times \text{ResBlock}(F)$
Bottleneck	$T/4 \times F$	$2 \times \text{ResBlock}(F)$
Conv1D	$T/4 \times D$	kernel=1, stride=1
Residual Vector Quantizer		
Quantization	$T/4 \times D$	Residual VQ
Decoder		
Input	$T/4 \times D$	Quantized Latents
Conv1D	$T/4 \times F$	kernel=3, stride=1
Bottleneck	$T/4 \times F$	$2 \times \text{ResBlock}(F)$
Stage 1	$T/2 \times F$	$2 \times \text{ResBlock}(F)$, Upsample
Stage 2	$T \times F$	$2 \times \text{ResBlock}(F)$, Upsample
Stage 3	$T \times F$	$2 \times \text{ResBlock}(F)$
Conv1D	$T \times C_{out}$	kernel=3, stride=1
Output	$T \times C_{out}$	Tanh activation

Table F. Architecture of the Animation Tokenizer. We denote the input sequence length as T and the feature dimension as $C_{in/out}$. The number of residual blocks per stage is set to 2. The base number of channels is $F = 1024$, and the latent dimension is $D = 128$. Downsampling and upsampling operations have a stride of 2.

speech (past) \rightarrow speech (current)). This helps the model learn the temporal dynamics of the modality.

- **Cross-Modal Generation Tasks:** The majority of our tasks fall into this category. The model learns to generate a target modality from one or more different source modalities (e.g., speech (current), identity (time-invariant) \rightarrow expression (current)).
- **Chained Generation Tasks:** The tasks are designed to be composable, enabling a chained generation pipeline in our "Thinking in Modality" (e.g., image (time-invariant) \rightarrow identity (time-invariant), then speech (current) \rightarrow expression (current), etc.). Our task suite includes all these intermediate steps to facilitate such chained inference.

This extensive set of 72 tasks, detailed in Table G, ensures that the model is exposed to a vast number of input-output combinations, fostering a deep multimodal understanding and enabling the generation of high-fidelity, holistic avatars.

D. Multimodal Data Details

In this section, we provide a detailed description of the data acquisition and preprocessing pipeline for the all modalities used in our model: description, script, speech, animation, semantic video and image/video. Our pipeline is designed

to extract temporally synchronized multimodal data from a large-scale video source, which are essential for training our holistic avatar generation model.

D.1. Description

The description modality provides a rich, structured representation of the person in the video. This modality is designed to capture a holistic set of attributes encompassing appearance, actions, and environmental context. To ensure consistency and comprehensiveness, we employ Gemini 2.5 Pro [11] for the annotation process. A detailed prompt, shown in Figure L, guides the model to analyze a video and return a structured JSON object containing all discernible attributes.

The resulting JSON object is organized into three primary keys: appearance, action, and environment.

- **appearance:** This category captures the subject’s physical characteristics. It includes static attributes such as gender, age_group, ethnicity, and body_build, as well as more detailed features like hair_color, hair_style, facial_features, and detailed descriptions of clothing and other physical_attributes.
- **action:** This section details the dynamic aspects of the subject’s performance. It describes the overall activity_type, emotional expression, and nuanced behaviors such as mouth_action, eyebrow_action, head_action, and

Output Modality	Input Modality Combinations
script (c)	[desc (t)], [script (p)], [speech (c)], [expr (c)], [semantic (c)]
speech (c)	[desc (t)], [desc (t), script (c)], [script (c)], [script (c), speech (p)], [speech (p)], [script (c), image (t)], [script (c), semantic (c)], [script (c), speech (p), semantic (c)], [id (t), expr (c)], [semantic (c)], [script (c), id (t)]
image (t)	[desc (t)], [speech (c)], [id (t)], [id (t), expr (t), pose (t)], [desc (t), id (t), expr (t), pose (t)]
identity (t)	[desc (t)], [desc (t), script (c), speech (c)], [speech (c)], [image (t)]
expression (c)	[desc (t)], [desc (t), script (c), speech (c), image (t), id (t)], [script (c)], [script (c), speech (c), id (t)], [speech (c)], [speech (c), id (t)], [speech (c), id (t), image (t)], [speech (c), image (t)], [semantic (c)], [expr (p), speech (c)]
pose (c)	[desc (t)], [speech (c)], [speech (c), id (t), expr (c)], [speech (c), expr (c), image (t)], [speech (c), id (t), expr (c), image (t)], [image (t), id (t), expr (c)], [image (t), expr (c)], [id (t), expr (c)], [semantic (c)]
semantic (c)	[desc (t)], [desc (t), script (c)], [desc (t), script (c), speech (c)], [desc (t), script (c), speech (c), id (t), expr (c), pose (c)], [desc (t), image (t)], [desc (t), script (c), speech (c), id (t), expr (c), pose (c), image (t)], [script (c)], [script (c), image (t)], [script (c), speech (c), id (t), expr (c), pose (c), image (t)], [speech (c)], [speech (c), id (t), expr (c), pose (c)], [speech (c), id (t), expr (c), pose (c), image (t)], [speech (c), image (t)], [speech (c), expr (c), pose (c), image (t)], [image (t)], [image (t), id (t), expr (c), pose (c)], [image (t), expr (c), pose (c)], [image (t), expr (c)], [id (t), expr (c), pose (c)], [semantic (p)], [semantic (p), speech (c)], [semantic (p), expr (c), pose (c)]
description (t)	[speech (c)], [image (t), semantic (c), speech (c)], [image (t), semantic (c), speech (c), script (c)], [image (t)], [image (t), semantic (c)], [id (t), expr (c), pose (c)]

Table G. Overview of the 72 Multimodal Training Tasks. The model is trained to predict the output modality from various input combinations. The state of each modality is indicated in parentheses: (c) for current, (p) for past, and (t) for time-invariant. For brevity in long combinations, we use abbreviations: desc (description), id (identity), and expr (expression).

gaze_direction. It also captures the overall emotion and energy_level conveyed.

- **environment:** This category provides context for the scene, describing the lighting_conditions, background_description, and the general scene_context (e.g., indoor/outdoor).

This structured approach ensures that our model is trained on a consistent and detailed descriptive modality, enabling it to generate holistic and high-fidelity avatars. An example of the generated JSON data is presented in Fig. K.

D.2. Script

The script modality is derived from word-level caption data, which includes precise start timestamps and durations for each word. This allows for fine-grained alignment between the text, speech, and video. When an audio-video clip is extracted, we query the caption data to find all words whose time intervals overlap with the clip’s duration. These selected words are then concatenated in their original order to form the final script that corresponds precisely to the spoken content within that segment. This method ensures that the script is accurately aligned with its corresponding audio and video, which is critical for training our multimodal

Label Name	Label Name	Label Name
background	hair	pupil
face	brows	iris
neck	lashes	sclera
ears	beard	clothes
upper_lip	teeth	glasses
lower_lip	tongue	headwear
nostrils	other_in_the_mouth	accessory

Table H. The 21 semantic labels used for generating semantic segmentation maps.

model.

The aforementioned process applies to our training data where precise word-level annotations are available. For our test sets, specifically CelebV-HQ [69] and HDTF [66], ground-truth captions are not provided. Therefore, we utilize OpenAI’s Whisper model [37] to transcribe the audio into text. This allows us to evaluate our model’s performance on datasets with automatically generated scripts, reflecting a more realistic, in-the-wild scenario.

D.3. Speech

The speech modality is processed to be tightly synchronized with the corresponding video segment. The raw audio track is first resampled to a standard 16 kHz sampling rate. To enhance signal quality and improve model robustness to acoustic variations, we apply a denoising model [62] to 50% of the audio samples, selected at random. The remaining 50% are left unchanged to improve the robustness of model. To align the audio with the video, we extract an audio segment corresponding to the sampled video clip using its timestamps. If the source audio is shorter than the target duration at the sampled point, we pad the segment with silence to ensure a consistent length across all samples.

D.4. Animation

The animation modality in our model is derived from 3D Morphable Model (3DMM) parameters [17], which provide a rich, structured representation of the human head’s geometry and dynamics. These parameters are not directly available in the raw video data and are obtained through a pre-processing step where a 3DMM is fitted to each video frame using an optimization-based approach [13]. This fitting process yields a set of continuous parameters for each frame, which contains facial expression, person-specific identity, head rotation, and head translation.

To make these continuous parameters suitable for our multimodal language model, we convert them into a sequence of discrete tokens. This tokenization process is crucial as it allows our model to handle animation in a manner

analogous to text. The process involves two main steps: normalization and vector quantization. First, we use pre-calculated mean and standard deviation of each parameter to normalize itself independently. Second, the normalized continuous parameters are quantized into discrete tokens using three separate, learned Vector Quantized-Variational Autoencoders [47] (VQ-VAEs). We use distinct VQ-VAEs for expression, identity, and pose (where pose is the concatenation of rotation and translation parameters). Each VQ-VAE has its own learned codebook, effectively creating a unique vocabulary for each animation component. This process maps the high-dimensional, continuous animation signals into compact sequences of discrete tokens. By tokenizing the animation parameters, we can seamlessly integrate them into our transformer-based MLLM architecture, enabling it to learn cross-modal associations between animation, script, speech, and video frames.

D.5. Semantic Video

For the semantic video modality, we process each frame to generate a semantic segmentation map. This provides our model with a context-efficient representation of video, particularly focusing on the human subject. We utilize the DINOv2 model [34] to parse segmentation, which delineates 21 distinct classes corresponding to key facial features, hair, and accessories. This fine-grained labeling scheme enables our model to learn detailed representations of the human head and upper body. The complete list of the 21 semantic labels is provided in Table H. This detailed decomposition is instrumental for the model to generate realistic textures and geometry for each part of the avatar, from the subtle nuances of eye components to various accessories.

D.6. Image/Video

Our video processing pipeline is designed to generate normalized, head-centric video clips. Initially, raw videos are decoded and uniformly downsampled to a frame rate of 30 frames per second (fps). To achieve a consistent, head-centric view, we first detect the facial landmarks to the face in each frame. From the 3DMM fit, we derive a bounding box that encompasses the face and a portion of the upper body. To ensure a stable view without jitter, we compute a common crop region based on the union of these bounding boxes across the entire video sequence. The size of this crop is randomly scaled to introduce variations in framing, from tight close-ups to wider shoulder-level shots. This cropped region is then resized to a final resolution of 256×256 pixels using bicubic interpolation with anti-aliasing.

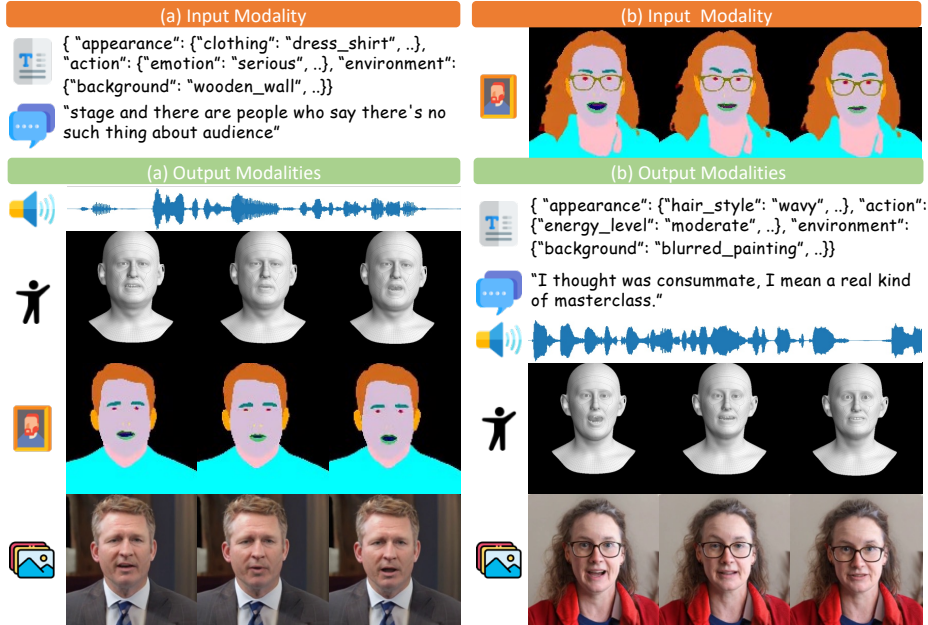


Figure H. **Multimodal Generation.** We show our model is capable of doing text or speech-to-all generation and can support a variety of cross-modality reasoning and generation tasks.

Methods/Metrics	FID↓	FVD↓
Ours w/o text cond	17.2310	32.3772
Ours w/o joint crossattention	22.7003	36.1064
Ours	16.8678	26.6860

Table I. We show the ablation study on the different condition ways to the diffusion model.

E. More Results

E.1. Multimodal Generation

We present additional qualitative results of our multimodal generation framework. As illustrated in Fig. H (a), when conditioned on a description of a subject (e.g., a man in a suit) and a corresponding script, our model successfully synthesizes all complementary modalities, including speech, animation, semantic segmentation, and the final RGB video. These generated modalities exhibit precise temporal synchronization, with the output video demonstrating high visual fidelity and strict alignment with the input conditions. Besides, in Fig. H (b), we demonstrate generation from semantic inputs; given a semantic video, our model synthesizes a photorealistic video that faithfully adheres to the semantic appearance and motion. Furthermore, the model demonstrates its understanding capabilities by accurately inferring the description, script, speech, and animation directly from the semantic video input.

E.2. Modality-specific Editing

We further demonstrate our model’s versatility in multimodal editing in Fig. I. In Fig. I (a), we perform script editing, where we synthesize a new talking video that articulates a modified script while faithfully preserving the subject’s original appearance and vocal identity. In Fig. I (b), we illustrate disentangled attribute editing by altering the speaker’s gender from male to female while retaining fine-grained attributes such as hairstyle and clothing. Notably, the model simultaneously adapts the generated voice to align with the modified visual appearance, demonstrating robust cross-modal consistency. Finally, Fig. I (c) depicts animation editing (face reenactment); by utilizing 3DMM coefficients extracted from a reference video, we drive the source subject to replicate the reference’s pose and expressions with high fidelity.

E.3. Comparisons with Unified Models.

Current unified models are not truly “holistic” in the context of digital human. While models such as Qwen-Omni [57] can understand multimodal inputs, their outputs are confined to text and audio. Similarly, Show-o2 [56] supports text, image, and video but omits audio. NExT-GPT [55], though capable of audio generation, produces environmental or musical sounds rather than intelligible speech. In contrast, Archon is the first model to learn the joint distribution of holistic human-centric modalities.

Video Understanding. We evaluate human talking video understanding against Qwen-Omni [57], a 30B Mixture-of-

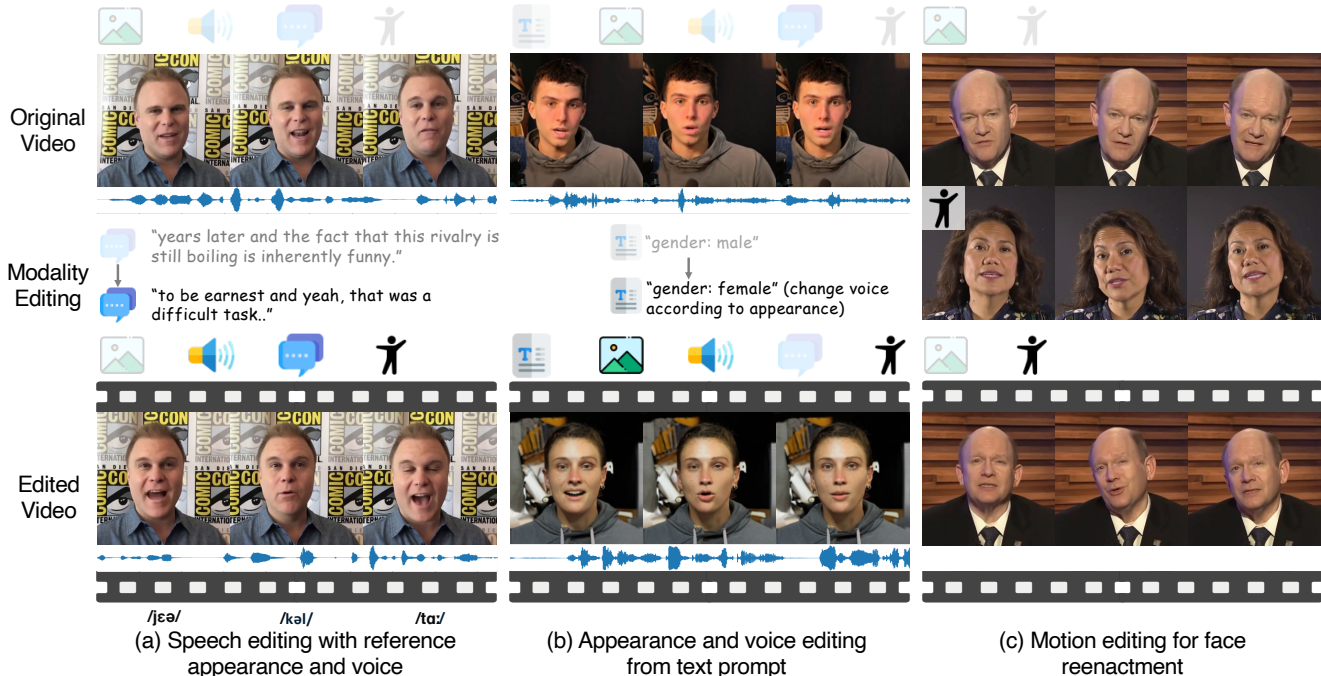


Figure I. **Modality-specific Editing.** We demonstrate that our model support editing multimodal input with remarkable flexibility - modifying arbitrary chosen modal while maintains the others untouched. The icons on the top showing the modalities used in the example, and the highlighted icons are the ones that are varied.

Experts model. The test set, drawn from HDTF [66], is annotated using Gemini3 [14] to provide ground-truth descriptions. The query 2prompt is shown in Fig. L and is also used for Qwen-Omni. Performance is measured by the average F1 score across all descriptive attributes, where precision P_s and recall R_s are derived from the cosine similarity of BGE embeddings [7]:

$$P_s = \frac{1}{|\mathcal{P}|} \sum_{p \in \mathcal{P}} \max_{g \in \mathcal{G}} \cos(\text{BGE}(p), \text{BGE}(g)),$$

$$R_s = \frac{1}{|\mathcal{G}|} \sum_{g \in \mathcal{G}} \max_{p \in \mathcal{P}} \cos(\text{BGE}(g), \text{BGE}(p)).$$

with \mathcal{P} and \mathcal{G} denoting the predicted and ground-truth attribute sets, respectively. Despite its compact 1B parameter size, Archon attains an F1 score of 0.90, which is comparable to the 0.93 achieved by the substantially larger Qwen-Omni model.

Text-to-AV. For talking video and audio synthesis from text, we compare with NEX-T-GPT [55], the most closely related unified model. Input prompts define human attributes and dialogue scripts, as shown on the left of Fig. J. We use Gemini [14] to translate this JSON-formatted description to natural language and input it to NEX-T-GPT. As illustrated in Fig. J, we synthesize significantly higher-quality video and audio than NEX-T-GPT. NEX-T-GPT produces visually corrupted video lacking recognizable facial features or motion,

along with unintelligible or silent audio. We generate high-fidelity talking head video that accurately reflects the provided description, with well-synchronized lip movements and clear audio corresponding to the input script.

E.4. Ablation of Semantic-driven Video Diffusion Model

We investigate the impact of different conditioning mechanisms on the video diffusion backbone, with quantitative results summarized in Tab. I. All ablations are performed on the held-out test split. Given the dense temporal nature of the semantic video input, we employ channel-wise concatenation with the noisy latents rather than cross-attention, adhering to computational memory constraints. In Sec. 3.3, we propose concatenating the reference image with its corresponding segmentation mask for cross-attention (“Ours”). This strategy establishes a structural bridge, facilitating the effective transfer of appearance from the reference to the synthesized video. We contrast this with a baseline that utilizes only the RGB reference image in the cross-attention module (“Ours w/o joint cross-attention”). As observed in Tab. I, the degradation in FID and FVD scores in the absence of segmentation image underscores their critical role in guiding the diffusion model to accurately map reference appearance to generated motion. Finally, we assess the contribution of textual prompts. The configuration “Ours w/o text cond” omits text embeddings from the cross-attention

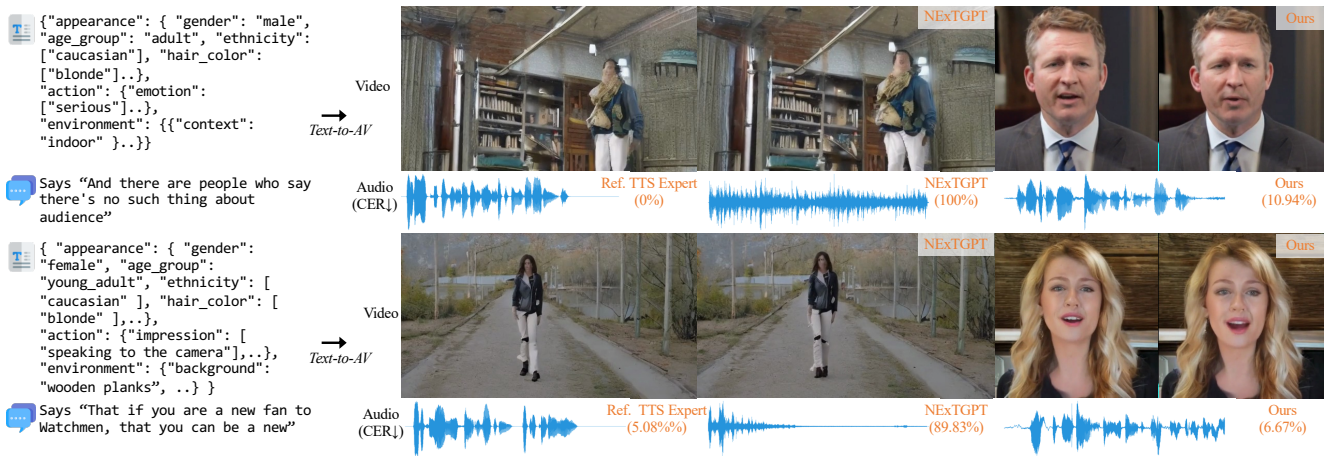


Figure J. **Text-to-AV Comparisons.** We present a comparative evaluation against NExT-GPT for the generation of audio and video from textual input (comprising both description and script).

layers. The resulting decline in metrics confirms that multi-modal conditioning is essential for maintaining high video fidelity.

```

{
  "appearance": {
    "gender": "male",
    "age_group": "adult",
    "ethnicity": ["caucasian"],
    "body_build": ["average"],
    "hair_color": ["black"],
    "hair_style": ["short"],
    "facial_features": ["none_discernible"],
    "clothing": {
      "upper_body": "button-down_shirt_over_t-shirt",
      "lower_body": "none",
      "footwear": "none",
      "accessories": ["watch", "ring", "bracelet"],
      "dominant_colors": ["black", "blue", "white", "red"]
    },
    "physical_attributes": {
      "visible_tattoos": "none",
      "visible_piercings": "none",
      "distinctive_marks": "none",
      "posture": "upright",
      "gait": "not_applicable",
      "physical_aids": ["none"]
    }
  },
  "action": {
    "activity_type": "speaking",
    "expression": "smile",
    "overall_impression": ["gesturing_with_hands_while_speaking", "raising_hands_to_chest_level", "making_a_fist"],
    "emotion": ["positive_and_engaging", "enthusiastic"],
    "energy_level": ["medium_to_high", "animated"],
    "mouth_action": ["wide_opening", "narrow_opening", "relaxed_lips", "pulling_of_lip_corners", "synchronization_and_precision_with_spoken_words"],
    "eyebrow_action": ["raising_inner_eyebrows", "raising_outer_eyebrows", "brow_furrowing"],
    "blink_frequency": "medium",
    "head_action": ["mostly_centered", "tilts_inquisitively", "nods_rhythmically", "amplitude_and_tempo_of_movements", "directional_changes_pitch/yaw/roll", "frequency_of_changes", "transitions_between_stillness_and_motion"],
    "eye_state": ["fully_wide_alert"],
    "gaze_direction": ["straight_ahead", "fixed_forward_focus"],
    "nonverbal_habits": ["habitual_eyebrow_flicks", "frequent_micro-nods", "timing_and_context_of_cues", "consistency_of_cues", "typical_amplitude_subtle_vs_pronounced"],
    "interactions": ["with_object_e.g._microphone/instrument", "none"],
    "props_used": ["microphone", "none"]
  },
  "environment": {
    "lighting_conditions": "bright",
    "background_description": "light_colored_wall_with_a_framed_certificate_and_a_model_of_a_watch_on_a_shelf",
    "time_of_day": "unknown",
    "weather_conditions": "indoor_not_applicable",
    "context": "indoor"
  }
}

```

Figure K. An example of the structured JSON description obtained from Gemini 2.5 Pro.

Enhanced Video/Image Analysis Prompt

You are an expert video and image analysis AI. Your task is to meticulously analyze a given video or sequence of images featuring a person performing, and extract all possible relevant attributes about the person, their actions, and the surrounding environment.

Critical Instruction for JSON Output

Your output MUST be a single, complete, and perfectly valid JSON object. Do NOT include any introductory or concluding text, explanations, or extraneous characters outside of the JSON. Ensure proper syntax, including all commas, brackets, and quotes.

Data Extraction Schema

Here's the information you need to extract, grouped into three main categories, and the precise JSON format you must adhere to. For attributes specified as lists (e.g., `body_build`, `hair_color`, `hair_style`, `facial_features`, `accessories`, `dominant_colors`, `physical_aids`, `interactions`, `props_used`, `overall_impression`, `Mouth_Action`, `Eye_brow_Action`, `Head_Action`, `Eye_State`, `Gaze_Direction`, `Nonverbal_Habits`), ensure you return a list containing ALL discernible attributes. The attribute values given below are just examples, but use them for inspiration. Attributes should be strings with underscores instead of space where necessary.

```
{
  "appearance": {
    "gender": "male/female/non-binary/unknown",
    "age_group": "child/preteen/teenager/young_adult/adult/older_adult/senior/unknown",
    "ethnicity": ["list_ethnicities_if_discernible", "caucasian", "asian", "african_american", "hispanic", "middle-eastern", "unknown", "etc."],
    "body_build": ["slim", "average", "athletic", "muscular", "heavy", "unknown"],
    "hair_color": ["black", "brown", "blonde", "red", "gray", "white", "green", "blue", "pink", "other", "unknown"],
    "hair_style": ["bald", "long", "short", "curly", "straight", "wavy", "..."],
    "eye_color": ["light_brown", "dark_brown", "light_blue", "..."],
    "eye_style": ["long_eyelashes", "short_eyelashes", "..."],
    "teeth": ["straight", "missing_teeth", "..."],
    "facial_features": ["glasses", "beard", "wrinkly_skin", "elastic_skin", "clean_skin", "sideburns", "mustache", "freckles", "..."],
    "clothing": {
      "upper_body": ["description_of_upper_garment_e.g._t-shirt/dress_shirt/blouse/hoodie/jacket/sweater/tank_top/sports_bra/suit/tie/none"],
      "lower_body": ["description_of_lower_garment_e.g._jeans/trousers/skirt/shorts/leggings/sweatpants/none"],
    },
    "physical_attributes": {
      "visible_tattoos": "description_of_tattoos_and_location_if_visible_e.g._full_sleeve_right_arm/small_design_neck/none",
    },
    ...
  },
  "action": {
    "activity_type": "dancing/singing/playing_instrument/speaking/acting/sports/walking/running/sitting/standing/other",
    "expression": "smile/frown/closed_mouth/etc.",
    "overall_impression": ["brief_descriptive_summary_of_the_performance", "e.g._head_turn_to_the_left", "e.g._raising_her_left_arm"],
    "emotion": ["description_of_general_energy_and_dominant_emotional_tone", "e.g._animated_and_joyful", "..."],
    "energy_level": ["overall_magnitude_of_emotional_display", "e.g._faint_micro-expressions_to_vivid_reactions", "e.g._consistently_low-key"],
    ...
  },
  "environment": {
    "lighting_conditions": "bright/dim/natural_light/artificial_light/backlit/etc.",
    "background_description": "detailed_description_of_the_background_e.g._blurred_trees/crowded_street/empty_white_wall",
    "time_of_day": "morning/afternoon/evening/night/unknown",
    "weather_conditions": "sunny/cloudy/rainy/snowy/indoor_not_applicable/etc.",
    "scene_context": "indoor/outdoor/stage/street/home/office/natural_environment/etc."
  }
}
```

Figure L. The part of the prompt provided to Gemini 2.5 Pro for video annotation.